
Biogeochemistry **69:** 37–62, 2004.

The role of down-slope water and nutrient fluxes in the response of Arctic hill slopes to climate change

EDWARD B. RASTETTER*, BONNIE L. KWIATKOWSKI, SÉVERINE LE DIZÈS and JOHN E. HOBBIE

*The Ecosystems Center, Marine Biological Laboratory, Woods Hole, MA 02543, USA; *Author for correspondence (e-mail: erastett@mbl.edu; fax: +1 508 457 1548)*

Received 29 November 2001; accepted in revised form 16 May 2003

Key words: Carbon–nitrogen interactions, Climate change, Ecosystem model, Hill-slope processes, Scaling, Spatial interactions

Abstract. The down-slope movement of water and nutrients should link plant and soil processes along hill slopes. This linkage ought to be particularly strong in Arctic ecosystems where permafrost confines flowing water near the surface. We examined whether these hill-slope processes are important in assessments of the responses of Arctic tundra to changes in CO_2 and climate using the Marine Biological Laboratory–General Ecosystem Model. Because higher rates of water flow decrease the distance over which nutrients must diffuse to the roots, down-slope vegetation is more productive under current conditions. In response to elevated CO_2 and a warmer, wetter climate, the relative increase in carbon stored in vegetation and soils was higher uphill, but the absolute increase was higher downhill. Very little of the increase in carbon anywhere on the hill slope resulted from an increase in total ecosystem nitrogen. Instead, the increases were associated with increases in vegetation C:N ratio (woodiness) and with the redistribution of nitrogen from soils (low C:N) to vegetation (high C:N). Because these changes are fueled by nitrogen already in place, the down-slope movement of nitrogen does not appear to be a major determinant of the responses of Arctic tundra to changes in CO_2 and climate.

Introduction

Hill-slope processes like the down-slope movement of water and nutrients are rarely considered when assessing the productivity of terrestrial ecosystems or their response to changes in the environment (but see Oberbauer et al. 1989; Shaver et al. 1991; Ostendorf and Reynolds 1993). Most studies that address hill-slope processes focus on the delivery of water and solutes to streams at the base of the hill rather than on the effects of these processes on the hill-slope ecosystems themselves (e.g., Hornberger et al. 1994; Preedy et al. 2001). However, as nutrients move down slope, they are repeatedly taken up, cycled through vegetation and soils, and released back into the soil solution. Hence nutrients tend to spiral down slope rather than flow directly to the stream at the base of the hill. This nutrient-spiraling concept (Newbold et al. 1981, 1982), which has proven so useful for analyzing productivity patterns in stream ecosystems, has never been applied to hill slopes; yet analogous processes clearly must occur, especially on slopes with strong lateral water movement (Marion and Everett 1989; Kling et al. 2000; Reiners and Driese 2001).

These hill-slope processes potentially could have important effects on the responses of terrestrial ecosystems to changes in the environment. For example, elevated CO_2 concentrations might increase nutrient demand up slope and thereby decrease down-slope nutrient flux and result in a lag or attenuation of the CO_2 response farther down slope. Alternatively, high rates of nutrient release up slope in response to warming might result in a faster and stronger response down slope. Do these types of interactions need to be taken into account to make reliable projections of the long-term ecosystem and landscape responses to changes in the environment?

Despite the potential importance of these hill-slope processes, they are never explicitly represented in regional or global simulations, largely because the computational costs are too high. Instead, these models extrapolate spatially by repeated and independent application of a plot-scale model to each location on a spatial grid (e.g., McGuire et al. 1992; Cramer et al. 1999; Williams et al. 2001; Le Dizès et al. 2003). Although the plot-scale model is typically parameterized based on data from experimental plots less than a few $100\,m^2$ in size, it is assumed to represent a far larger area (100–$10{,}000\,km^2$) without accounting for plot-to-plot interactions like the movement of water and nutrients on hill slopes. Spatial processes are sometimes implicitly incorporated by modeling individual vegetation types (e.g., Jenkins et al. 1999) or topographic units (e.g., Reiners et al. 1998; White et al. 1998) separately, but this implicit approach cannot capture the dynamics associated with plot-to-plot interactions. Thus, the spatial patterns arising from these regional and global model applications are the result of the spatial variations in the data used to drive the model (e.g., climate, soils, vegetation) and not the result of spatial interactions among simulated plots.

Even without an explicit representation of hill-slope and other spatial processes, regional models often capture the broad spatial pattern of productivity. For example, Schloss et al. (1999) compared estimates of the global pattern of net primary production from several models to satellite-based estimates and found generally high spatial correlations at a 0.5° latitude $\times$ 0.5° longitude resolution. On a more regional scale, Le Dizès et al. (2003), using the same model we employ below, found that the spatial patterns in modeled and satellite-based estimates of productivity in a catchment in northern Alaska were highly correlated at a $30\,km \times 30\,km$ resolution ($r^2 = 0.8$–0.9). This corroboration of models at coarse spatial scales suggests that hill-slope and other spatial processes can be ignored. However, these comparisons are based on near-steady-state conditions and cannot address the decade-to-century-scale transient responses of ecosystems to elevated CO_2 concentrations, climate change, or other long-term environmental change (Rastetter 1996). Because of the potential time lags associated with the down-slope movement of N, hill slope process could have important effects on these transient responses (Reiners and Driese 2001).

In this paper, we analyze how the down-slope movement of water and N affects responses of Arctic tussock tundra to changes in atmospheric CO_2 and

climate. Because water and dissolved nutrients are held near the surface by permafrost, this down-slope movement is thought to be particularly important to the productivity of tundra ecosystems (Shaver et al. 1991). Our approach is theoretical, based on a simple, conceptual hill slope consisting of a sequence of moist tussock tundra plots linked through the transport of water and N down slope. Plant and soil processes on each plot are simulated using a model of ecosystem C–N interactions (Marine Biological Laboratory–General Ecosystem Model, MBL-GEM III; Le Dizès et al. 2003).

Material and methods

Our modeling exercise focused on hill slopes covered by the moist tussock tundra typical of the northern foothills of the Brooks Range in northern Alaska. Several characteristics make these systems attractive objects of study: (1) They are the most common vegetation type in northern Alaska (Bliss and Matveyeva 1992); (2) They have been intensively studied, especially at the Arctic Long-Term Ecological Research (LTER) site near Toolik Lake, Alaska (68°38′N, 149°36′W: Shaver and Chapin 1986, 1991; Grulke et al. 1990; Giblin et al. 1991; Oechel et al. 1992; Chapin et al. 1995; Chapin and Shaver 1996; Hobbie and Chapin 1998); (3) Because of the large store of N in soil organic matter, they have a very high potential for increased nutrient availability and primary production in response to a warmer climate (Nadelhoffer et al. 1992, 1997); and (4) They have been simulated with several ecosystem models, including ours, so parameter sets are available (e.g., Ostendorf and Reynolds 1993; McKane et al. 1997a,b; Rastetter et al. 1997; Hobbie et al. 1998; Le Dizès et al. 2003).

Tussock tundra covers most gentle hill slopes in northern Alaska. The soils are always moist and unevenly covered with a dense organic mat, 30–50 cm thick, overlaying silt mineral soil and permafrost (Marion and Oechel 1993). The depth of soil thaw typically ranges from 30 to 55 cm. Total soil C above the maximum depth of thaw generally increases down slope and varies from about 10 to 27 kg C m^{-2} (Giblin et al. 1991). Total plant biomass and net primary production (excluding fine roots) are, respectively, about 385 g C m^{-2} and 80 g C m^{-2} $year^{-1}$ (Shaver and Chapin 1991), but productivity can be 2 – 3 times higher in water tracks (Chapin et al. 1988). Productivity of tussock tundra in northern Alaska is strongly N limited (Shaver and Chapin 1986), and the N limitation is much stronger than potential limitation by low light or low temperature (Chapin and Shaver 1985; Chapin et al. 1995).

Model description

The MBL-GEM III is a process-based, plot-scale model of the interactions of C and N in terrestrial ecosystems. The general structure of the model has been described in several papers (Rastetter et al. 1991; McKane et al. 1997a).

Le Dizès et al. (2003) describe MBL-GEM III in detail and test its regional predictions of productivity against satellite data ($r^2 = 0.8$–0.9). Only a brief, general description will be given here followed by a description of the modifications made for this particular application.

The MBL-GEM III simulates, on an annual time step, plot-level photosynthesis and N uptake by plants, allocation of C and N to foliage, stems, and fine roots, respiration in these tissues, turnover of biomass through litter fall, and decomposition of litter and soil organic matter. The model was calibrated to run on mean-July maximum and minimum daily air temperature, mean-July daily irradiance, total growing-season precipitation, mean-annual CO_2 concentration, and annual N inputs in deposition. A major feature of the model is that vegetation in the model acclimates to changes in the environment to maintain a nutritional balance between C and N. For example, environmental changes that stimulate photosynthesis (e.g., increased CO_2 or higher irradiance) result in an increase in the relative allocation of C and N to fine-root growth, which, in turn, stimulates N uptake. Similarly, environmental changes that stimulate N uptake (e.g., increased available N) increase the relative allocation of C and N to foliage growth, which stimulates C uptake. The C:N ratio of litter determines how it is partitioned among organic matter fractions that differ in relative turnover rates. The rates of decomposition and N mineralization also depend upon soil temperature and moisture. Of significance in wet tundra soils, the effect of soil moisture on soil processes is hump shaped, increasing to an optimum and then declining as soils become waterlogged (Flanagan and Veum 1974).

McKane et al. (1997a,b) used the GEM to analyze responses of tussock tundra to 9-year manipulations of nutrients (N + P fertilization), temperature (greenhouses), and light (shade houses). Of particular importance to the present study, the model was able to simulate the observed $\sim 40\%$ increase in stem (woody) and leaf biomass associated with a fertilizer-induced shift in community structure. The community changed from one with an approximately even distribution of graminoid, evergreen, and deciduous shrub biomass to one dominated by deciduous shrub biomass. A similar transition to woodier vegetation is thought to be occurring in northern Alaska in response to a warmer climate (Sturm et al. 2001). An analogous spatial transition to more productive, woodier vegetation also occurs along the gradient between tussock tundra and water tracks (Shaver and Chapin 1991; Gough et al. 2000). Our main goal is to determine if the interaction of this spatial transition with down-slope movements of water and nutrients might have ramifications on the responses of tussock-tundra landscapes to changes in CO_2 and climate.

Spatial interactions among plots

We simulated 101 contiguous $1\,m \times 1\,m$ plots on a transect running along the water flow path down a hill slope covered with tussock tundra. The simulated

plots were linked through the movement of water and dissolved inorganic N down the slope. Dissolved organic N (DON) losses are 2–3 times higher than inorganic N losses (10–15 μM v.s. ~5 μM, Keisuke Koba and Yuriko Yano, personal communication). However, DON was assumed to be relatively inert and so could not stimulate plant production down-slope and provide the spatial linkages central to our analysis. We have therefore ignored DON fluxes down slope. To simplify the analysis, we assumed a hill slope with uniform aspect and slope so that there were no convergent or divergent water flow paths. Permafrost beneath the tundra assures that no water is lost to deep percolation. Therefore, all the water flowing out of one plot was assumed to run into the next plot down slope. The flux of inorganic N between adjacent plots equaled the water flux times the concentration of dissolved inorganic N in the up-hill plot. Other forms of N transport including organic N and long-distance N transport between nonadjacent plots associated with animal movements and wind-blown litter were not considered. We also ignore denitrification in our simulations because its rate is very low in arctic ecosystems of northern Alaska (Chapin et al. 1980, Schimel et al. 1996).

Soil moisture and discharge

Because of the annual time step in the GEM, we had to derive an estimate of summer soil moisture and total summer water flux from plot to plot. We therefore developed a simple daily-time-step, tipping-bucket model of the water balance for the 101 contiguous 1 m × 1 m plots. We assumed a 10% slope, which is typical of the steeper hills covered with tussock tundra near Toolik Lake (USGS topographic maps). As with the annual model, we assumed the plots were sealed at the bottom by permafrost, that the uphill plot had no inputs except from the atmosphere and snow melt, and that each successive plot drained directly into the next plot down slope so there was no convergent or divergent flow of water and no deep percolation.

We used a Priestley and Taylor (1972) evapotranspiration model with a coefficient (α) of 0.67, which is consistent with other studies on the Alaskan North Slope (Wilson et al. 2002). We assumed 85% porosity and 39% field capacity, by volume (Bridgham et al. 2001), and frozen-soil water content of 35% (= 15 mm below field capacity in a 370 mm soil) to account for wintertime desiccation (Kane 1997). We assumed the maximum depth of thaw was 370 mm for all plots, the average 1990–2000 August thaw depth in tussock tundra near Toolik Lake, and we imposed a seasonal pattern to the depth of thaw based on soil-temperature profiles at Toolik Lake (Arctic LTER 2002).

Down-slope discharge was simulated based on the slope and hydraulic conductivity:

$$Q = K\frac{\mathrm{d}z}{\mathrm{d}x}h\frac{y}{A}$$

where Q is the down-slope discharge (mm day^{-1}), K is the hydraulic conductivity (m day^{-1}), dz/dx is the slope of the hill (assumed = 0.1 m m^{-1}), h is the depth of standing water above the depth of thaw (mm), y is the width of a plot (= 1 m) and A is the area of a plot (= 1 m^2). To calculate h, we assumed that all the soil above the water table was at field capacity:

$$h = \frac{(W - fz_T)}{(\rho - f)}$$

where W is the total soil water (mm), f is the field capacity (fraction by volume = 0.39), ρ is the porosity (= 0.85), and z_T is the depth of thaw (mm), which changes through the season.

We calibrated the model using 1996 flow and meteorological data from Imnavait Creek (Kane and Hinzman 1998), which is about 10 miles north of Toolik Lake. We did not expect our simple transect model to simulate individual hydrographs, which are strongly governed by the complex geomorphology of a catchment, particularly on saturated areas near the stream channel. However, we wanted the model to roughly match the seasonal pattern of cumulative discharge. Our simulations began on May 27 as the soils began to thaw and therefore after the beginning of snowmelt. About two-thirds of the discharge in the calibration data occurred during the first 15 days of our simulation and was clearly associated with snowmelt. To account for this snowmelt, we added a total of 147 mm of water to the precipitation entering each of the 100 plots during the first 13 days of the simulation; we found that the best fit was obtained by decreasing the amount of water added each day exponentially from about 39 mm on day 1 of the simulation to about 1 mm on day 13. We then calibrated the hydraulic conductivity using stream-flow data for the rest of the season. To match the cumulative discharge, we estimate that the value of K was about 8 m day^{-1}, which is consistent with measured hydraulic conductivity for peat soils (e.g., Almendinger and Leete 1998). Comparison of modeled to measured cumulative discharge for Imnavait Creek indicated that we overestimate, on average, by about 3% through the summer ($r^2 = 0.99$).

Based on this model, we derived a relationship between average growing-season soil moisture and the total active-season water inputs (snowmelt plus summer precipitation plus flow from up slope). Because of the changing depth of thaw, we calculated a weighted-mean soil moisture using the depth of thaw for the weighting:

$$W_m = z_{Tmax} \sum_{t=1}^{S} \frac{W(t)}{z_T(t)}$$

where W_m is the mean soil moisture (mm), z_{Tmax} is the seasonal maximum depth of thaw (mm), S is the number of days with thawed soil, $W(t)$ is the liquid water content of the soil on day t (mm), and $z_T(t)$ is the depth of thaw on

day t (mm). We then related this mean soil moisture to total active-season water inputs to the plot using a nonlinear regression based on data generated with the daily model ($r^2 = 0.99$):

$$W_m = 0.47\, Q_{in}^{0.49} + 118$$

where Q_{in} is the total active-season water inputs (mm year^{-1}). We also derived a relationship relating total active-season water discharge to the total active-season water inputs ($r^2 = 1$):

$$Q_{out} = 0.9975\, Q_{in} - 95$$

where Q_{out} is the down-slope discharge. The difference between water inputs and discharge accounts for both evapotranspiration and water left in the soil when the soil freezes in the fall. We used these equations for mean soil moisture and annual discharge in the annual-time-step GEM simulations.

Water-flow effects on N uptake by roots

The model had to be modified to account for the effects of moving water on N availability to roots. At steady state, a plot at the bottom of our transect would receive roughly 100 times the N inputs that enter a plot at the top of the transect. However, this increased N flux is not enough to explain the productivity gradient observed along hill slopes (e.g., highly productive water tracks) because this increase in N flux is accompanied by a proportional increase in water flux. Thus, the concentration of N in soil water, which is what determines uptake by roots, is about the same all along the transect. However, flowing water will increase N concentration near the root surface because it overcomes the depletion zone around roots and thereby decreases 'the distance over which the nutrients must otherwise diffuse' (Chapin et al. 1988; Schimel et al. 1996). To account for this effect, we adjusted the concentration of N at the root surface based on the water flux out of each plot:

$$[N]_{root} = [N]_{aq}(1 - 0.5\, e^{-0.02 Q_{out}})$$

where $[N]_{root}$ and $[N]_{aq}$ are the N concentrations at the root surface and in the soil solution away from the root, respectively. The 0.5 and 0.02 values were selected to yield roughly a doubling of productivity from top to bottom of the hill slope (Chapin et al. 1988).

Model calibration

The specific data and steps that were used to calibrate the MBL-GEM III were described in Le Dizès et al. (2003) and the general approach is described in

detail in McKane et al. (1997a). Briefly, the model was calibrated to biomass and production of moist acidic tussock tundra based on a 9-year study reported by Chapin et al. (1995) in which plots at Toolik Lake were experimentally manipulated with fertilizer, greenhouses, and shade houses. Results from an experiment that doubled atmospheric CO_2 in chambers at the same site (Oechel et al. 1992) were also used to calibrate the model. In the calibration procedure a subset of rate parameters was adjusted until a single parameter set was found that was simultaneously consistent with the responses of all these experimental manipulations. The average error in the model predictions of biomass (exclusive of fine roots) over all treatments was $\sim \pm 10\%$ (zero-intercept regression of observations on model predictions slope = 0.98, $r^2 = 0.57$). The full parameter set for moist tussock tundra is reported in Le Dizès et al. (2003).

Input data set and simulation protocol

Our simulations were based on historic and projected climate data for the years from 1921 to 2100 (Figure 1). We used temperature and precipitation data from the Arctic LTER for the years 1989–2000 (Arctic LTER 2002), which we augmented with historical and projected data extracted from a 0.5° latitude $\times$ 0.5° longitude, gridded dataset compiled by McGuire et al. (2000). The historical records in this data set were derived from data reported by Jones (1994), Hulme (1995), and Legates and Willmott (1990a,b). The projected climate was based on a Hadley Center CM2 model simulation that included the combined effects of greenhouse gases and sulfate aerosols (Mitchell et al. 1995). We added 147 mm of snowmelt to the summer precipitation to be consistent with the water-budget model described above (Section on *Soil moisture and discharge*). We estimated mean maximum and minimum July temperatures for Toolik Lake based on a regression relating the mean July temperatures in the 1989–2000 Arctic LTER data to the McGuire et al. (2000) data ($r^2 = 0.44$). We then used these temperature data to estimate mean July daily irradiance from a three-parameter Bristow and Campbell (1984) model derived by Williams et al. (2001). The historical CO_2 data were derived from ice-core measurements and atmospheric CO_2 observations (Enting et al. 1994). For the projected CO_2 data, we assumed a linear doubling of CO_2 concentrations in the next 100 years (Figure 1). We assumed inorganic N inputs in deposition to be $0.0141\ g\,N\,m^{-2}\,year^{-1}$ throughout the simulation, which is the average summer deposition at Toolik Lake for the years 1989–1999 (Arctic LTER 2002; winter deposition is assumed to run off with snow melt because of the frozen soil).

In addition to the precipitation and N deposition, each of the simulated plots, except the first one, also received water and N from up hill. The total water input to a plot equaled the discharge from the nearest plot up hill, plus the precipitation on the plot itself. Similarly, the total N input equaled the N leaching from the nearest up hill plot plus the N deposition.

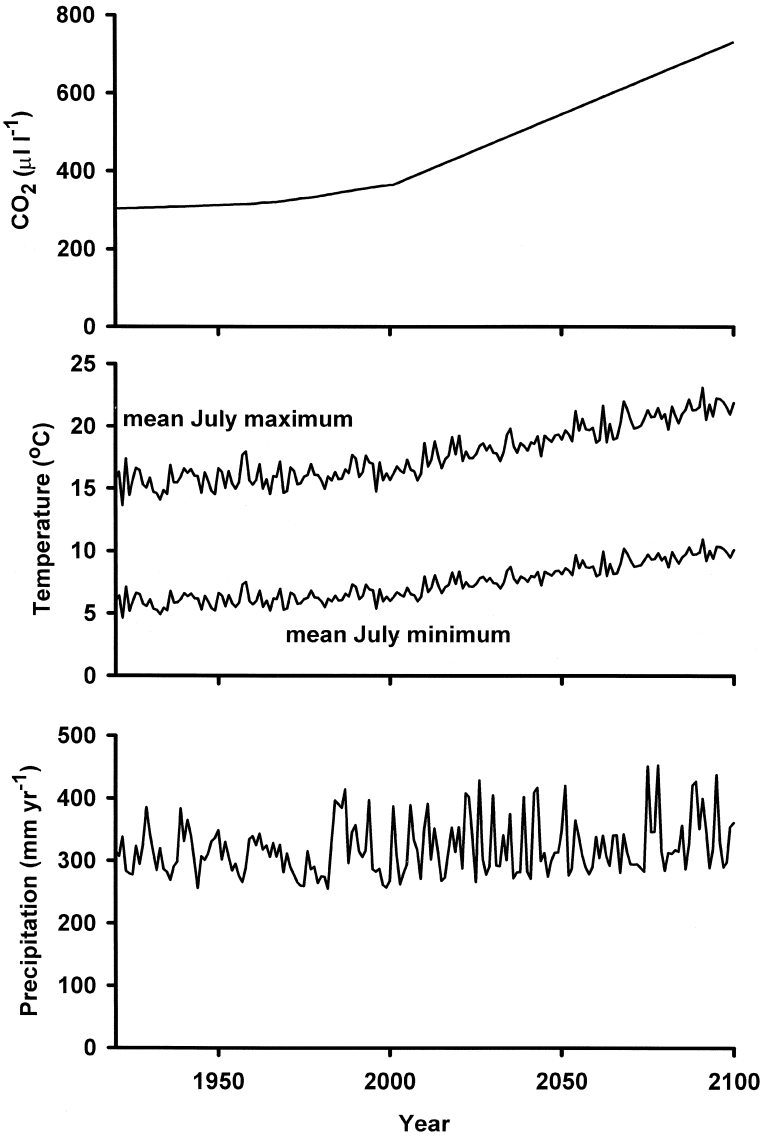

Figure 1. Time-series data used to drive the GEM III. Data were compiled to represent historical and projected future climate at the Arctic Long-Term Ecological Research site near Toolik Lake, Alaska.

To eliminate transients associated with initial conditions, we began each simulation with a 2000-year spin-up period during which the climate, N deposition, and CO_2 concentration were held constant at their respective mean values for the years 1921–1930. Because humus C and N require a very long

time to reach steady state (>10,000 years), we adjusted these values by trial and error until all plots along the transect were near steady state (Net Ecosystem Production (NEP) < 0.005 g C m^{-2} $year^{-1}$).

Two simulations were run. First, to assess the time lags associated with down-slope movement of water and N without the confounding effects of a varying climate, we ran a simulation in which climate, N deposition, and CO_2 concentration were held constant but 1% of the humus was removed from all plots along the transect and the hill slope was allowed to recover for 100 years. Second we ran a simulation in which climate, N deposition, and CO_2 concentration varied from 1921 through 2100, as described above.

Analysis of C–N interactions

A key assumption of our analysis was that, for strongly N-limited ecosystems like the Alaskan tundra, changes in C storage strongly interact with changes in the N cycle (Schimel 1990; Rastetter et al. 1992; Shaver et al. 1992; McKane et al. 1995). Through the coupling between C and N uptake by plants and between soil respiration and net N mineralization, the model incorporates several biogeochemical constraints on the C budget imposed by the N cycle. Therefore, to help interpret the simulated changes in ecosystem C, we partitioned the response among four factors related to C–N interactions (Rastetter et al. 1992). The first factor relates to the amount of C that would be gained or lost based solely on the simulated gain or loss of N by the ecosystem, but assuming that the relative distribution of N between plants and soils and the C:N ratios of plants and soils did not change. The second and third factors relate to the changes in ecosystem C associated with the simulated changes in the C:N ratios of plants and soils, but assuming no change in total ecosystem N or in the relative distribution of N between plants and soils. The fourth factor relates to the change in ecosystem C associated with changes in the relative distribution of N between plants and soils, but assuming no change in total ecosystem N or in plant or soil C:N ratios. A redistribution from soils to plants usually results in an increase in ecosystem C because the C:N ratio of soils is generally lower than that of plants. These four factors can interact synergistically (e.g., a redistribution of N from soils to plants that also increase in C:N ratio), so an interaction term is also included in the analysis. Each factor (and their interaction) was mathematically described as an independent contributor and the sum of the calculated contributions accounted for the total change in ecosystem C stocks (Rastetter et al. 1992). We used these equations to analyze how the four factors and their interaction regulated the predicted spatial and temporal changes in ecosystem C stocks along the hill slope.

To help understand the climatic influence on these four factors, we calculated cross correlations between the time series for each factor and the time series for temperature and precipitation. These cross correlations can

be confounded by long-term trends in the data, which can be associated with secondary, rather than direct, affects on the ecosystem. We therefore removed the trend in all time series by differencing (i.e., by replacing a time series x_t with $y_t = x_t - x_{t-1}$; Young 1984). The analysis is therefore based on the change in the value of a characteristic relative to its value the previous year. We present cross correlations only relating changes in the four factors to changes in temperature and precipitation in the same year. No significant correlations were found for lags of one year or more when the cross-correlation estimates were corrected for autocorrelation in the respective time series.

Results and discussion

Steady-state spatial patterns

All of our simulations began with soils and vegetation near steady state with the 1920s climate. Under our assumptions of no convergent or divergent water flow, the average soil water content near steady state increased down slope from 126 mm at the top to 178 mm at the bottom, with half that increase occurring in the first 30 m. The steady-state water flux out of our simulated plots increased from 220 mm $year^{-1}$ at the top of the hill to 19,668 mm $year^{-1}$ 100 m down slope. The down-slope movement of water increased the rate of N delivery to the plots from 0.0141 g N m^{-2} $year^{-1}$ at the top of the hill (i.e., the annual atmospheric N deposition rate) to 1.41 g N m^{-2} $year^{-1}$ 100 m down slope (Figure 2). However, because the flow of water also increased down-slope, the concentration of inorganic N in soil water only increased 13%.

The steady state N uptake by vegetation, net primary production (NPP), and net N mineralization from soils increased down slope by 126, 106, and 126%, respectively. These increases occurred despite a 16% decline in the relative rate of soil organic N turnover associated with the increase in waterlogging (Figure 2; Flanagan and Veum 1974; Schimel et al. 1996). The increase in N uptake resulted from the effect of flowing water on diffusion gradients near roots rather than from the small increase in N concentration in soil water (Chapin et al. 1988). This increase in N uptake fueled higher NPP down slope and higher litter inputs of N to soils, which in turn had to be matched by higher net N mineralization rates at steady state.

Vegetation biomass and soil organic matter (SOM) increased along the slope by 112 and 169%, respectively (Figure 3). The increase in vegetation biomass was the result of higher NPP. There was also an 11% increase in the fraction of vegetation biomass in woody tissues, which is about the increase in woodiness observed after 3 years of fertilization (McKane et al. 1997a). The large increase in SOM was a consequence of both the increase in litter associated with higher NPP and with the slow soil-turnover rates in the wet soils (Flanagan and Veum 1974).

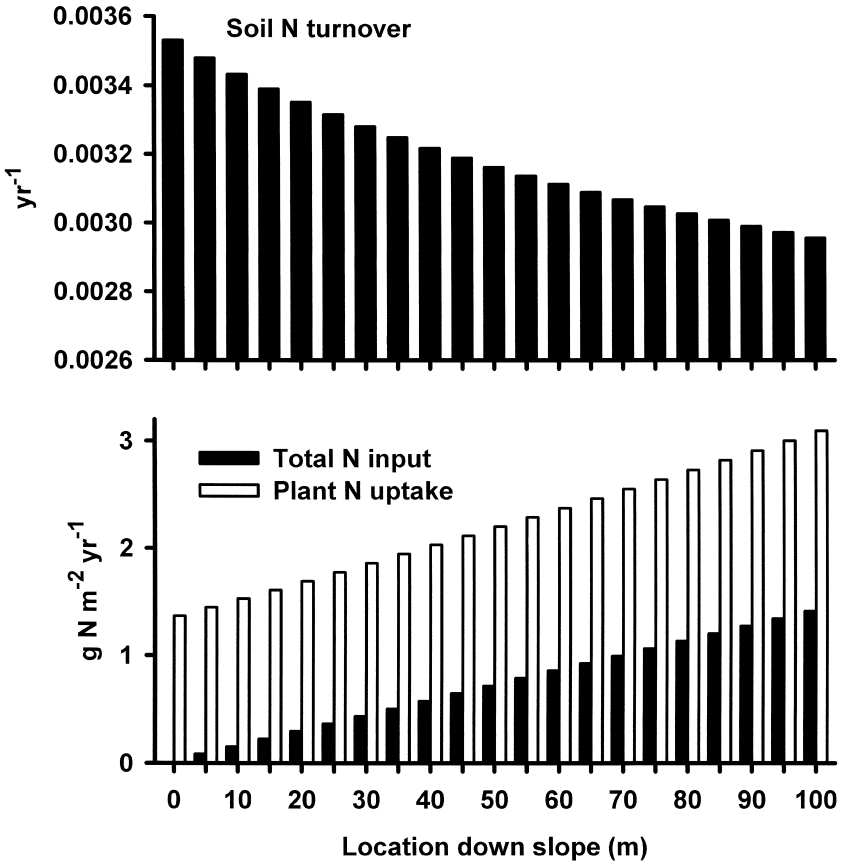

Figure 2. Relative rates of N turnover in soil and the rates of N uptake by plants and of N supply from the atmosphere plus ground water for simulated plots along a 100 m transect down an Arctic hill slope covered with tussock tundra.

Down-slope time lags: response to humus removal

Following the simulated removal of 1% of the humus, ecosystem processes and properties along the hill slope underwent a series of oscillations (Figure 4). The timing of the peaks and troughs in these oscillations indicate that the recovery at the base of the slope lagged behind the recovery at the top of the slope and that the magnitude of the lag increased by about 0.3 years for each year of recovery (Table 1). The oscillations were associated with the cycling of N within each plot and the lag in timing along the hill slope was associated with the disruption of the down-slope N flux among plots.

Immediately upon removal of 1% of the humus, net N mineralization dropped by 0.62% at all locations along the slope (the absolute decrease was larger down slope than at the top because the amount of humus was larger).

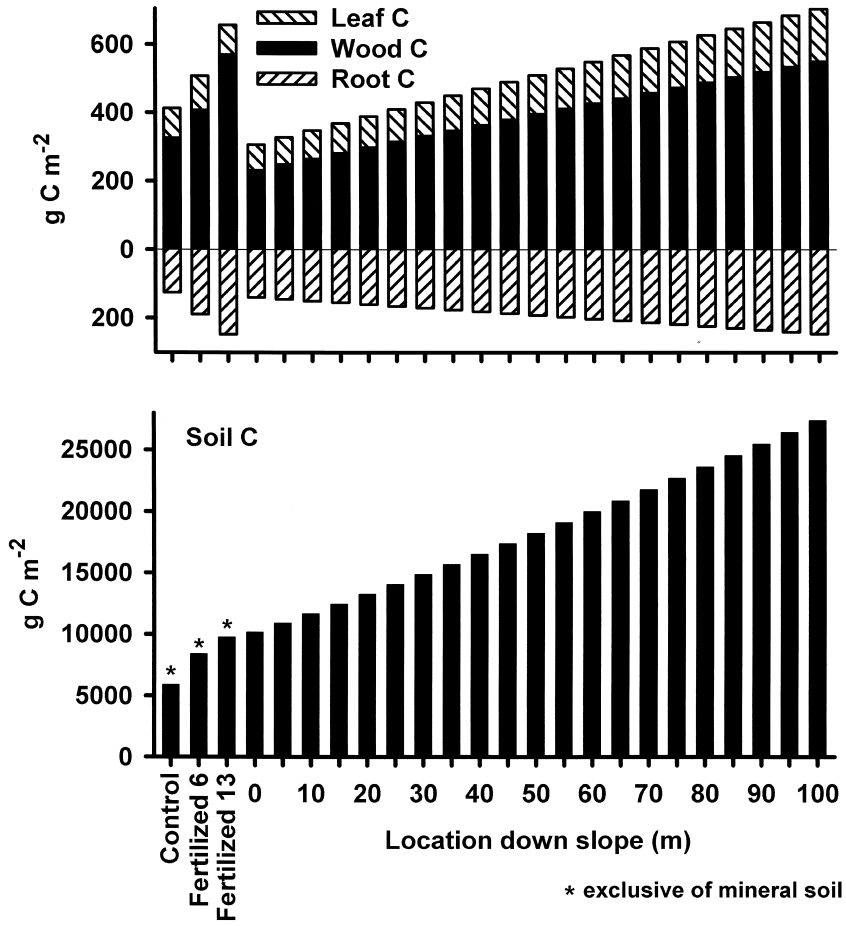

Figure 3. Amounts of C in plant tissues and soils in simulated plots along a 100 m transect down an Arctic hill slope covered with tussock tundra. Data are for plots at steady state with the average 1920–1930 climate. Also shown for comparison are data from a control plot and two experimental plots fertilized with $10\,g\,N\,m^{-2}\,year^{-1}$ and $5\,g\,P\,m^{-2}\,year^{-1}$ for 6 and 13 years at the Arctic LTER site (data courtesy of Gaius R. Shaver, personal communication).

The decrease in N mineralization resulted in a decrease in the available N in soils, which in turn resulted in a decrease in N uptake by plants, in N immobilization by soil microorganisms, and in the flux of N down slope. The effects of these decreases propagated through the vegetation and soils on each plot and also propagated down slope. This feedback resulted in further declines in NPP, vegetation biomass, soil organic matter, soil respiration, and N mineralization.

About 3 years after the humus removal, the concentration of available N and the rate of N flux down slope reached minima at all locations on the slope

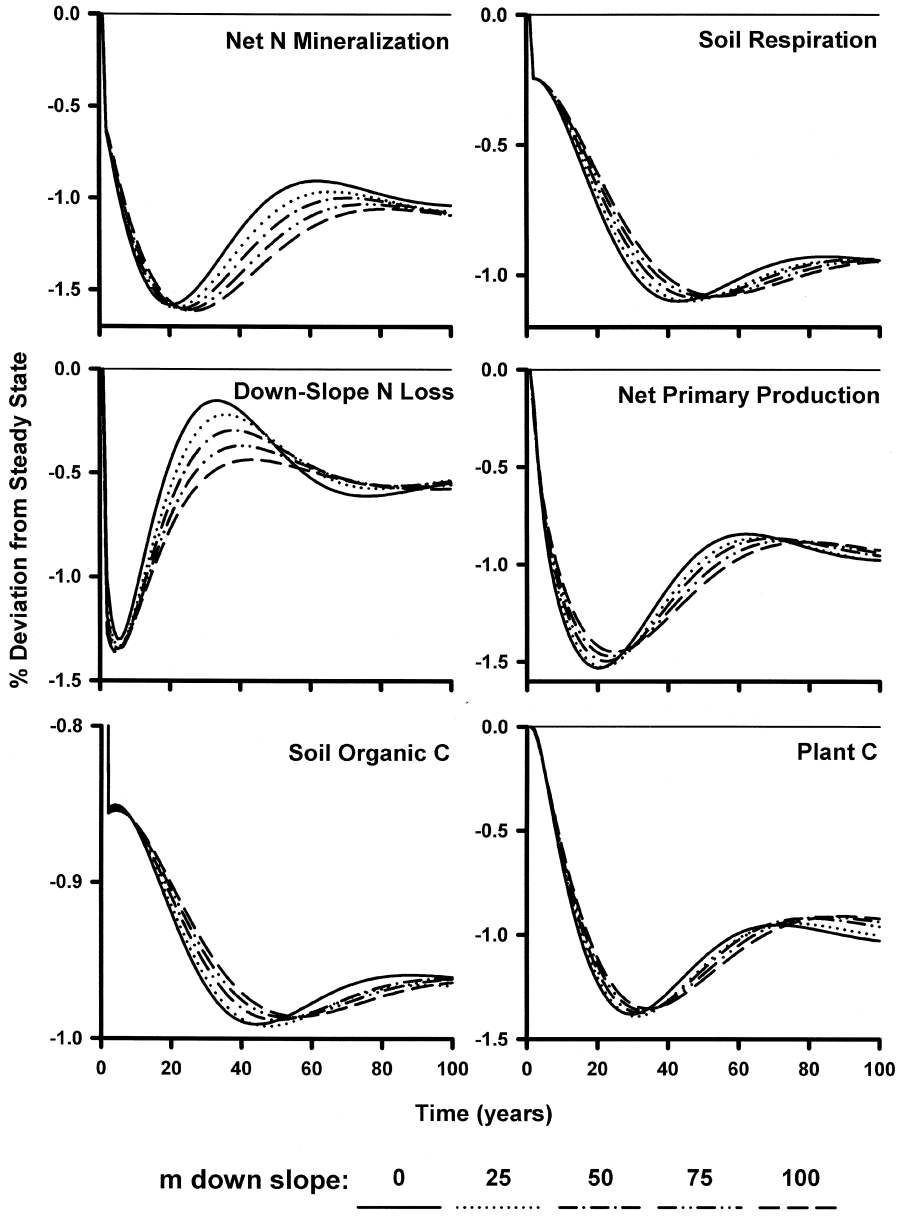

Figure 4. Simulated changes in ecosystem properties at five locations along a 100 m transect down an Arctic hill slope following a 1% removal of humus. Data are expressed as a percent deviation from the steady state values at the respective locations on the transect.

Table 1. Time and magnitude of the peaks and troughs in the oscillations of simulated ecosystem characteristics at the top and base of a hill slope following a 1% humus removal. Timing indicates time since humus removal. Lag is the lag in timing from top to base of the hill slope.

Timing		Lag	% Decrease from steady state		Peak or trough	Ecosystem characteristic
Top	Base		Top	Base		
2	2	0	0.85	0.85	P	Soil organic matter
3	3	0	1.30	1.37	T	Available N
3	3	0	1.30	1.37	T	Down-slope N flux
18	23	5	1.53	1.45	T	Net primary production
18	25	7	1.58	1.62	T	Net N mineralization
18	25	7	1.59	1.61	T	N uptake
27	34	7	0.96	0.96	P	Humus
28	32	4	1.38	1.35	T	Plant C
31	41	10	0.15	0.44	P	Available N
31	41	10	0.15	0.44	P	Down-slope N flux
41	52	11	1.10	1.08	T	Soil respiration
41	54	13	0.99	0.99	T	Soil organic matter
60	77	17	0.84	0.89	P	Net primary production
60	79	19	0.91	1.06	P	Net N mineralization
60	79	19	0.90	1.06	P	N uptake
69	87	18	0.95	0.91	P	Plant C
74	92	18	0.61	0.58	T	Available N
74	92	18	0.61	0.58	T	Down-slope N flux

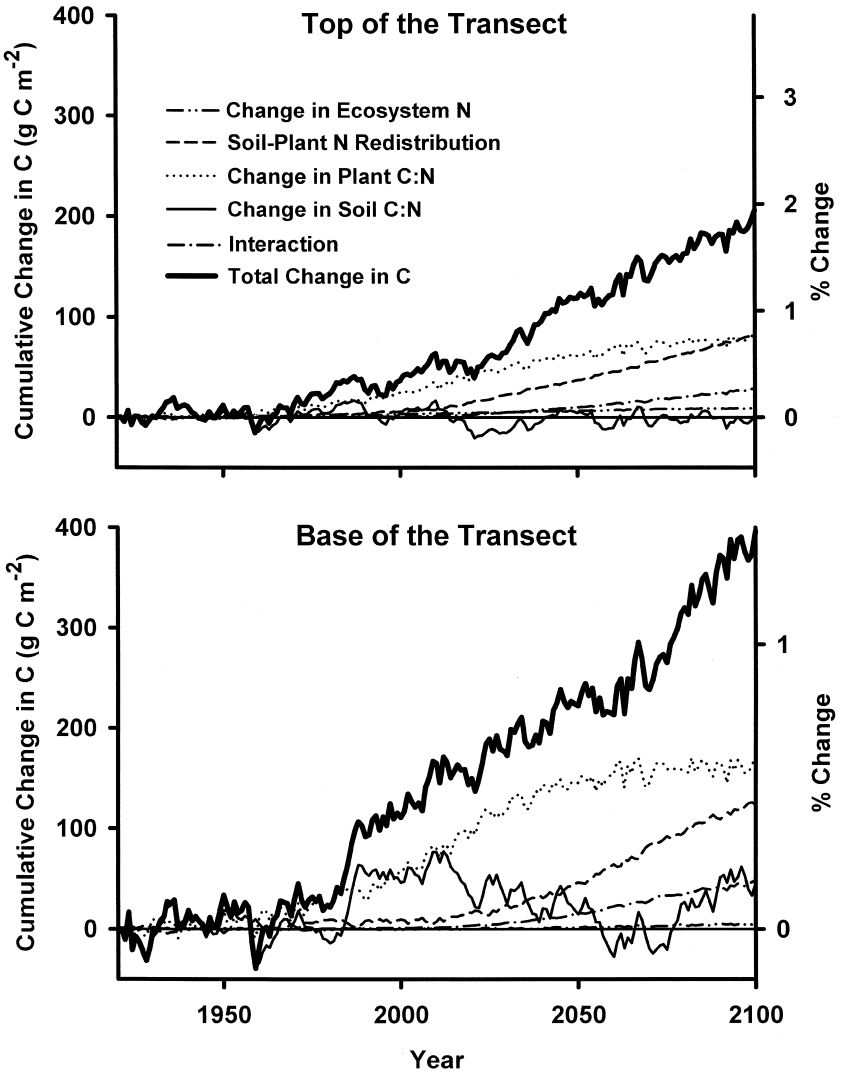

Figure 5. Simulated responses of tussock tundra to changes in climate and CO_2 concentration at the top and base of a 100 m transect down an Arctic hill slope. Shown are the cumulative net changes in total-ecosystem C since 1920 and the partitioning of those changes in C among four factors and their synergistic interaction. The four factors associate the changes in ecosystem C with: (1) net changes in total ecosystem N, (2) redistribution of N between soils (low C:N) and plants (high C:N), (3) changes in the C:N ratio of plants, (4) changes in the C:N ratio of soils, and (5) the interactions among these four factors. The axis to the right quantifies the changes as a percent of the total ecosystem C in 1920 at the respective locations on the transect.

(Figure 4, Table 1). This reversal in the trajectory of N availability was the result of lower vegetation biomass and the consequent decrease in N uptake rather than of a recovery in N mineralization rates, which continued to decline. Despite this reversal, the down-slope N flux remained well below the steady-state rate beyond the end of the 100-year simulation. The down slope plots could not recover fully until this supply of N from uphill was restored, thus the lag in the recovery between the top and base of the slope continued to increase.

Because of the very long time constants, especially associated with soil processes in the Arctic, our simulations indicate that the system had barely begun to recover from the 1% humus removal even after 100 years. At that time, humus was still about 0.97% below steady state even at the top of the slope. At that rate, the plot at the top of the hill would only have recovered 2/3 of the humus loss after 3000 years. Because all other ecosystem properties were tied to humus by the N cycle, their full recovery was similarly slow. Because down-slope plots depend not only on N cycled within the plot, but also on N released from all the plots above them, their recovery would be several centuries slower.

Responses to climate change

In response to the 1920–2100 CO_2 and climate scenario we simulated, C accumulated in the ecosystem all along the hill slope (Figure 5). The absolute amount of C sequestered in the ecosystem increased down slope, with the base of the slope sequestering about twice as much C as the top (396 v.s. 205 $g\,C\,m^{-2}$). However, the relative increase in ecosystem C was higher at the top of the slope (1.9%) than at the base (1.4%). Vegetation biomass increased all along the slope throughout the simulation, but with a somewhat faster increase during the projected period (2000–2100) relative to the historic period (1921–2000). The absolute increase in vegetation biomass was higher down slope (269 $g\,C\,m^{-2}$ at the top, 487 $g\,C\,m^{-2}$ at the base), but again the relative increase was higher at the top of the slope (60%) than at the base (51%). The simulated soil C oscillated between gains and losses during the historic period, but there was a consistent C loss for the projected climate. Again the absolute changes were greater, but relative changes smaller, at the base of the slope ($-91\,g\,C\,m^{-2}$ or 0.3%) than at the top ($-63\,g\,C\,m^{-2}$ or 0.7%).

The largest contributing factor to the increase in C all along the slope was an increase in the C:N ratio of vegetation (from ~ 52 to $\sim 61\,g\,C\,g^{-1}$ N). Between 40.5% (top) and 43.8% (base) of the total change in ecosystem C was attributable to this increase (Figure 5). Although the relative contribution of this factor was nearly constant along slope, the underlying cause for the change in vegetation C:N ratio differed. At the top of the slope, about 64% of the increase in ecosystem C attributable to an increase in vegetation C:N ratios was associated with an increase in woodiness and the remaining 36% was associated with an increase in the C:N ratio of individual tissues. At the base of the

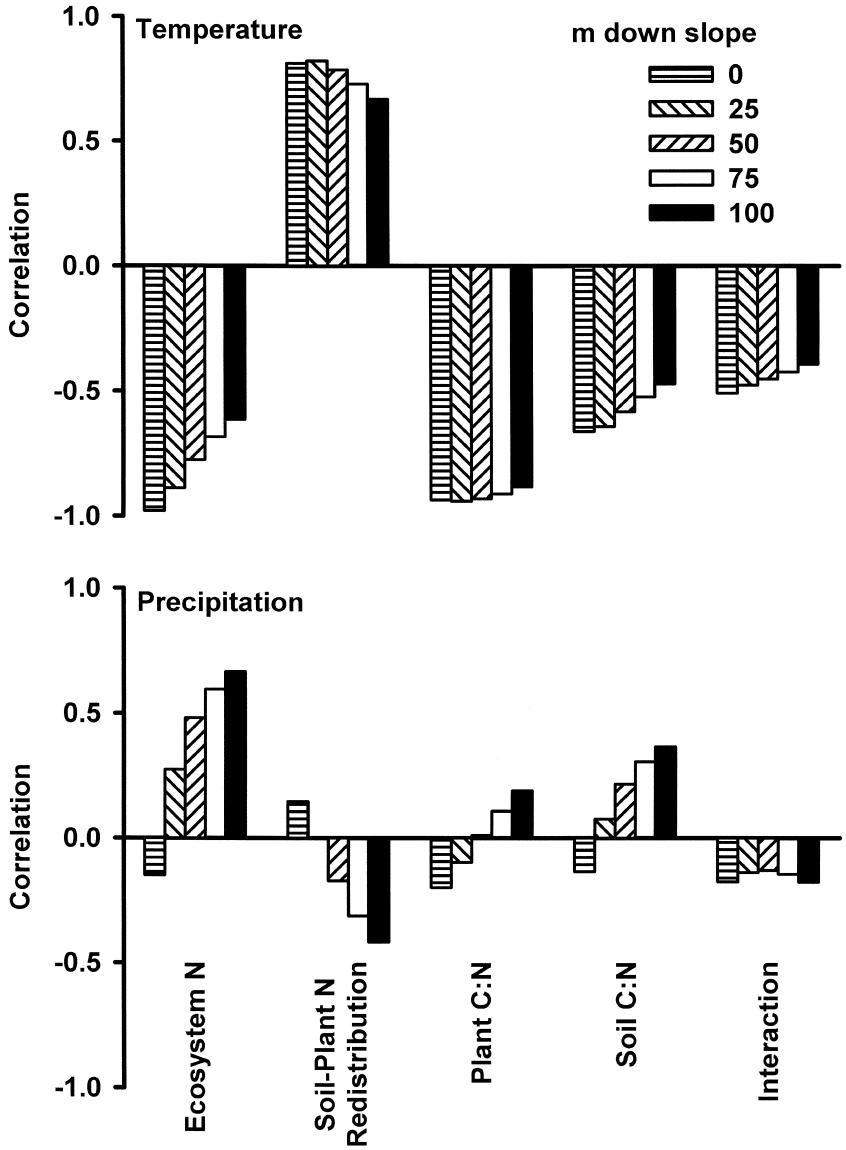

Figure 6. Correlations between climate and four factors relating changes in ecosystem C to properties of the ecosystem N budget at five locations along a 100 m transect down an Arctic hill slope. Long-term trends in the time series for temperature, precipitation, and the four factors plus their interaction were first removed by differencing (i.e., by replacing a time series x_t with $y_t = x_t - x_{t-1}$).

slope, only 48% of the increase was associated with increased woodiness and 52% with increasing tissue C:N ratios. The higher tissue C:N resulted from the stimulation of photosynthesis by elevated CO_2 concentrations. The long-term increase in woodiness resulted from generally higher fertility associated with faster N cycling in the warmer climate.

The cross correlation analysis on the de-trended time series indicated that the short-term change in vegetation C:N ratio in response to temperature was in the opposite direction (Figure 6). The correlation between the change in plant C:N ratio and the change in temperature in the same year was strongly negative everywhere along the slope; the C:N ratio tended to decrease in warm years because of higher respiration rates and higher rates of N supply from soils. The short-term effect of precipitation on vegetation C:N ratio was weak, but wet years tended to decrease the C:N ratio at the top of the slope and increase it at the base. The decrease in C:N ratios at the top of the hill was associated with a positive correlation between precipitation and temperature in the data ($r = +0.27$). Thus, the decrease in plant C:N ratio in wet years at the top of the hill was due to temperature-induced increases in respiration and N mineralization. The increase in plant C:N ratios at the base of the slope was due to inhibition of mineralization in the wet soils (moisture has minimal effect on photosynthesis in these wet soils).

The net movement of N from soils (with a C:N of $\sim 26\,g\,C\,g^{-1}$ N) to vegetation (with a C:N of $\sim 52\,g\,C\,g^{-1}$ N) accounted for 39% of the increase in ecosystem C at the top of the slope and for 31% at the base, and was the second most important of the four factors we analyzed (Figure 5). This net redistribution could be attributed to the long-term warming in the simulations. Warmer temperatures sped up the rate of N mineralization, and hence the supply of N to the vegetation, but had no direct effect on litter production and the return of N to the soil. Thus, the net redistribution of N was from soils to vegetation. Our time-series analysis indicated that the effect of short-term fluctuations in temperature was consistent with these long-term trends; in warm years, N tended to be redistributed from soil to vegetation (Figure 6). However, this temperature effect was somewhat weaker in the wet soils at the base of the slope than in the mesic soils at the top. Because of inhibition of N mineralization by waterlogging, the redistribution of N from soils to vegetation tended to decrease in wet years low on the hill slope. The slight increase in N redistribution from soil to vegetation in wet years at the top of the slope was again the result of the correlation between temperature and precipitation.

The contribution of changes in soil C:N ratio to the total change in ecosystem C varied throughout the simulation, but had no net trend at the top of the slope and only a weak positive trend at the base (Figure 5). The long-term increase in temperature should tend to decrease the soil C:N ratio by stimulating microbial processing of organic matter. However, the long-term increase in plant production increased the production of litter, which had a higher C:N ratio than soil, and thereby countered the temperature effect on soil C:N. Nevertheless, the short term relation between temperature and soil C:N was in

the opposite direction, as indicated by our time series analysis (Figure 6); the short-term stimulation of microbial processes did decrease the soil C:N ratio in warm years. Precipitation inhibited microbial processes during wet years at the base of the slope, increasing the soil C:N ratio. The slight decrease in soil C:N ratios at the top of the slope in wet years was again the result of the correlation of precipitation with temperature.

Our simulations indicated that very little of the ecosystem C gain was associated with an increase in the total amount of N in the plots anywhere along the slope. The top of the slope only gained 0.34 g N m^{-2} (0.09%) and the base only 0.2 g N m^{-2} (0.02%). If the plant and soil C:N ratios and relative distribution of N between plants and soils were kept constant at their initial 1921 values, the gains in N could account for C gains of only 9 g C m^{-2} at the top of the slope and 5 g C m^{-2} at the base (Figure 5). Although these gains in N were small, they nevertheless reflect the spatial interaction on the hill slope. The 0.34 g N m^{-2} accumulated at the top of the slope represented over 13% of the N deposition on that plot over the 180-year simulation. Under steady-state conditions, all of that N would have moved down slope. Thus, in response to the climate change, the upper plots removed N that would otherwise flow into lower plots. This removal of N means that the potential for sequestering C by accumulation of N decreased down slope. At the end of the simulation, the whole hill slope was accumulating about 0.25 g N $year^{-1}$ (or 0.0025 g N m^{-2} $year^{-1}$). This slow accumulation would have long-term consequences on ecosystem C storage, but would require thousands of years to fully materialize.

In the short term, faster rates of mineralization did result in a C loss associated with a loss of N in warm years (Figure 6). As with the gain in ecosystem C associated with the redistribution of N from soils to vegetation, the effect of temperature on N loss decreased down slope because the absolute effect of temperature on N mineralization was lower in waterlogged soils. The changes in ecosystem C associated with gains and losses in N were also apparent in the short-term effects of precipitation (Figure 6); in wet years, N tended to be lost from plots at the top of the slope, washed down slope, and taken back up in plots lower on the slope.

Conclusions

In our simulations, the down-slope movement of N mediated the potential for biogeochemical coupling along the hill slope. However, because N was strongly limiting and the external supply of N very low, the rate of N movement down slope relative to the rate of within-plot N recycling was very slow. Near the top of the slope, about 100 times as much N was recycled within a plot as was moving down slope. At the base, the recycled N was over twice that moving down slope. The spiraling length, the distance down slope that N travels each time it cycles through the ecosystem (Newbold et al. 1981, 1982), was therefore very short. Spiraling length can be calculated as the residence time of the N in

soil water times the velocity of water moving down slope. As an upper limit, we estimated the residence time of available N based on net N mineralization and N uptake by plants alone (i.e., ignored microbial immobilization and the abiotic exchange of N with soil particles). Using the average discharge velocity on the slope, we calculated a maximum spiraling length of about 0.26 m (stream spiraling lengths are on the order of 10–100 m). The residence time of the full N cycle on a plot was about 325 years, thus N moved only 0.26 m every 325 years on average. Equivalently, it would take, on average, over 125,000 years for an atom of N to move 100 m down our simulated hill slope.

To further assess the N-mediated coupling on the hill slope, we ran two ancillary simulations in which N deposition was increased to $5\,g\,N\,m^{-2}\,year^{-1}$ in the plot at the top of the slope or in the plot half way down the slope. At steady state, N movement into and out of all the plots down slope of the treated plot would have been increased by $5\,g\,N\,m^{-2}\,year^{-1}$. However, this steady state would require thousands of years to achieve. In the short term (<10 years), there was a pulse of N that moved down slope soon after the fertilization was initiated. At the top of the slope, this pulse was strongly attenuated to less than $0.1\,g\,N\,m^{-2}\,year^{-1}$ above background within 2 m. At mid-slope, the pulse was attenuated to slightly more than $0.1\,g\,N\,m^{-2}\,year^{-1}$ above background within 5 m. These results suggest that the coupling was stronger down slope where there was more water movement between plots. The results at the top of the slope explain why plots that have been fertilized at a rate of $10\,g\,N\,m^{-2}\,year^{-1}$ for 6–20 years at the Arctic LTER site (Shaver and Chapin 1986; Chapin et al. 1995) have very well defined boundaries in terms of standing biomass and there are no obvious plumes of fertility below the experimental plots. Our results are somewhat at odds with the observations of Marion and Everett (1989) who added $380\,g\,N\,m^{-1}$ (as slow-release fertilizer) into a trench cut along a transverse transect across a water track and found as much as $1\,mg\,N\,L^{-1}$ 6 m down slope. However, their study was in a water track, rather than on tussock tundra, and therefore their study site had higher water flow rates than in our simulations. As our simulations indicate, this higher water flux should result in stronger spatial coupling.

Our simulations of the 180-year response to past and projected changes in CO_2 concentration and climate indicate that spatial coupling associated with down-slope N movement is not an important factor for tussock-tundra hill slopes. The down-slope linkages were more obvious in our simulation of a 1% loss of humus and undoubtedly underlay the simulated responses to CO_2 and climate. However, on the timescale of our CO_2 and climate simulations, the effects of down slope N movement were very small relative to the effects of the within-plot N cycle. On longer timescales, the effects of down-slope N movement would be more apparent. For example, the increase in tissue C:N ratios indicates that the vegetation was still severely N limited even after the net redistribution of N from soils to vegetation. Litter from these high-C:N-ratio tissues also had a high N-immobilization potential and thereby sustained N limitation on plants. Assuming no further changes in the amount or the tissue

distribution of C in vegetation after 2100, about 1.71 g N m^{-2} would have to be accumulated by the vegetation to restore the initial C:N ratios of the tissues. At the rate that the ecosystem sequestered N in the simulations, and ignoring any net N immobilization into soils, it would take 682 years to restore the C:N ratios of plant tissues. That recovery would require 1100 years to restore the C:N ratios of both plants tissues and soils. Our humus-removal simulations indicated that in such a recovery, the base of the slope would lag well behind the top. While setting up the simulations for this study, we found that a 2000-year spin-up time was not enough to establish a steady state in the humus component of our model, which indicates that the 1100-year recovery time is probably very conservative. In any case, the dynamics associated with spatial linkages along the hill slope were very subtle and slow relative to the dynamics associated with the within-plot N interactions.

The Arctic landscape is comprised of a mosaic of vegetation types (heath, tussock tundra, wet sedge tundra, water tracks). Shaver et al. (1991) speculated that the patterns on this landscape are at least in part due to the movement of nutrients on hill slopes. Our results suggest that the patterns are more strongly associated with the underlying hydrology than the transport of nutrients across the landscape. Thus, the differences in vegetation and soils along our simulated hill slope, and their response to changes in CO_2 concentration and climate, were associated with the effects of soil water content on microbial processes and with the effects of flowing water on the diffusion to roots of N already in place, not with the movement of N down slope. If our results are robust, then landscape or regional-scale predictions of the response of Arctic ecosystem to changes in CO_2 and climate should be straightforward; the first step would be to use a topographically based hydrologic model (e.g., Beven and Kirkby 1979; Beven and Wood 1983; Ostendorf et al. 1996; Stieglitz et al. 1999) to predict soil moisture and the rate of water flow on the landscape, and then the second step would be to overlay an ecosystem model onto these predictions. There should be no need to account for spatial coupling associated with nutrient transport because the within-plot nutrient dynamics will dominate the responses, at least on a 200-year time scale.

Acknowledgements

Funding was provided by grants from the National Science Foundation (NSF-DEB 9810222, NSF-DEB 0108960, NSF-OPP 9732281, NSF-ATM 0221835).

References

Almendinger J.E. and Leete J.H. 1998. Regional and local hydrogeology of calcareous fens in the Minnesota River Basin, USA. Wetlands 18: 184–202.

Arctic LTER 2002. Online data base. Web site: http://ecosystems.mbl.edu/ARC/

Beven K.J. and Kirkby M.J. 1979. A physically based variable contributing area model of basin hydrology. Hydrol. Sci. Bull. 24: 43–69.

Beven K.J. and Wood E.F. 1983. Catchment geomorphology and the dynamics of runoff contributing areas. J. Hydrol. 65: 139–158.

Billings W.D., Luken J.O., Mortensen D.A. and Peterson K.M. 1982. Arctic tundra: a source or sink for atmospheric carbon dioxide in a changing environment. Oecologia 53: 7–11.

Bliss L.C. and Matveyeva N.V. 1992. Circumpolar arctic vegetation. In: Chapin F.S. III, Jefferies R.L., Reynolds J.F., Shaver G.R. and Svoboda J. (ed) Arctic Ecosystems in a Changing Climate. Academic Press, New York, pp. 59–90.

Bridgham S.D., Ping C.-L., Richardson J.L. and Updegraff K. 2001. Soils of northern peatlands: histosols and gelisols. In: Richardson J.L. and Vepraskas M.J. (eds) Wetland Soils, Genesis, Hydrology, Landscapes, and Classification. Lewis Publishers, Boca Raton, pp. 343–370.

Bristow K.L. and Campbell G.S. 1984. On the relationship between incoming solar radiation and daily maximum and minimum temperature. Agric. For. Meteorol. 31: 159–166.

Chapin F.S. III and Shaver G.R. 1985. Individualistic growth response of tundra plant species to environmental manipulations in the field. Ecology 66: 564–576.

Chapin F.S. III and Shaver G.R. 1996. Physiological and growth responses of arctic plants to a field experiment stimulating climatic change. Ecology 77: 822–840.

Chapin F.S. III, Miller P.C., Billings W.D. and Coyne P.I. 1980. Carbon and Nutrient budgets and their control in costal tundra. In: Brown J., Miller P.C., Tieszen L.L. and Bunnell F.L. (eds) An arctic ecosystem: The coastal tundra at Barrow, Alaska. US/IBP synthesis Series 12, Dowden, Hutchinson, and Ross, Inc., Stroudsburg, Pennsylvania, USA, pp. 458–482

Chapin F.S. III, Fetcher N., Kielland K., Everett K.R. and Linkins A.E. 1988. Productivity and nutrient cycling of Alaskan tundra: enhancement by flowing soil water. Ecology 69: 693–702.

Chapin F.S. III, Shaver G.R., Giblin A.E., Nadelhoffer K.J. and Laundre J.A. 1995. Responses of arctic tundra to experimental and observed changes to climate. Ecology 76: 694–711.

Cramer W., Kicklighter D.W., Bondeau A., Moore B. III, Churkina G., Nemry B., Ruimy A., Schloss A.L. andthe participants of the Potsdam NPP model intercomparison. 1999. Comparing global models of terrestrial net primary productivity (NPP): Overview and key results. Global Change Biol. 5 (Suppl 1): 25–34.

Enting I., Wigley T. and Heimann M. 1994. Future emissions and concentrations of carbon dioxide: key ocean/atmosphere/land analyses. CSIRO Division of Atmospheric Research Technical Paper, 31, 120 p.

Flanagan P.W. and Veum A.K. 1974. Relationship between respiration, weight loss, temperature and moisture in organic residues on tundra. In: Holding A.J., Heal O.W., Maclean S.F. Jr. and Flanagan P.W. (eds) Soil Organisms and Decomposition in Tundra. Swedish IBP Committee, pp. 249–277.

Funk D.W., Pullman E.R., Peterson K.M., Crill P.M. and Billings W.D. 1994. Influence of water table on carbon dioxide, carbon monoxide, and methane fluxes from taiga bog microcosms. Global Biogeochem. Cycles 8: 271–278.

Giblin A.E., Nadelhoffer K.J., Shaver G.R., Laundre J.A. and McKerrow A.J. 1991. Biogeochemical diversity along a riverside toposequence in artic Alaska. Ecol. Monogr. 61: 415–435.

Gough L., Shaver G.R., Carroll J., Royer D. and Laundre J.A. 2000. Vascular plant species richness in Alaskan arctic tundra: the importance of soil pH. J. Ecol. 88: 54–66.

Grulke N.E., Riechers G.H., Oechel W.C., Hjelm U. and Jaeger C. 1990. Carbon balance in tussock tundra under ambient and elevated atmospheric CO_2. Oecologia 83: 485–494.

Hastings S.J., Luchessa S.A., Oechel W.C. and Tenhunen J.D. 1989. Standing biomass and production in water drainages of the foothills of the Philip Smith Mountains, Alaska. Holarctic Ecol. 12: 304–311.

Hobbie S.E. and Chapin F.S. III 1998. The response of tundra plant biomass, aboveground production, nitrogen and CO_2 flux to experimental warming. Ecology 79: 1526–1544.

Hobbie J.E., Kwiatkowski B.L., Rastetter E.B., Walker D.A. and McKane R.B. 1998. Carbon cycling in the Kuparuk basin: plant production, carbon storage, and sensitivity to future changes. J. Geophys. Res. 103: 29,065–29,073.

Hornberger G.M., Bencala K.E. and McKnight D.M. 1994. Hydrological controls on dissolved organic carbon during snowmelt in the Snake River near Montezuma, Colorado. Biogeochemistry 25: 147–165.

Hulme M. 1995. A historical monthly precipitation data set for global land areas from 1900 to 1994 gridded at 3.75×2.5 resolution. Climate Research Unit, University of East Anglia, Norwich, UK

Jenkins J.C., Kicklighter D.W., Ollinger S.V., Aber J.D. and Melillo J.M. 1999. Sources of variability in net primary production predictions at a regional scale: a comparison using PnET-II and TEM 4.0 in northeastern US forests. Ecosystems 2: 55–570.

Johnson L.C., Shaver G.R., Giblin A.E., Nadelhoffer K.J., Rastetter E.B., Laundre J.A. and Murray G.L. 1996. Effects of drainage and temperature on carbon balance of tussock tundra microcosms. Oecologia 108: 737–748.

Jones P.D. 1994. Hemispheric surface air temperature variations: a reanalysis and an update to 1993. J. Climate 7: 1794–1802.

Kane D. 1997. The impact of hydrologic perturbations on Arctic ecosystems induce by climate change. In: Oechel W.C., Callaghan T., Gilnanov T., Holten J.I., Maxwell B., Molau U. and Sveinbjornsson B. (eds) Global Change and Arctic Terrestrial Ecosystems. Springer, New York, pp. 63–81.

Kane D.L. and Hinzman D. 1998. Meteorologic and hydrologic data sets, Kuparuk River Watershed, northern Alaska, USA. National Snow and Ice Data Center/World Data Center for Glaciology, Boulder, CO, USA. Digital Media. http://nsidc.org/data/catalog.html

Kling G.W., Kipphut G.W., Miller M.C. and O'Brien W.J. 2000. Integration of lakes and streams in a landscape perspective: the importance of material processing on spatial patterns and temporal coherence. Freshwater Biol. 43: 477–497.

Le Dizès S., Kwiatkowski B.L., Rastetter E.B., Hope A., Hobbie J.E., Stow D. and Daeschner S. 2003. Modeling biogeochemical responses of tundra ecosystems to temporal and spatial variations in climate in the Kuparuk River Basin (Alaska). J. Geophys. Res. Atmos. 108 (D2): 8165, doi: 10.1029/2001JD000960.

Legates D.R. and Willmott C.J. 1990a. Mean seasonal and spatial variability in global surface temperature. Theor. Appl. Climatol. 41: 11–21.

Legates D.R. and Willmott C.J. 1990b. Mean seasonal and spatial variability in gauge-corrected, global precipitation. Int. J. Climatol. 10: 11–127.

Marion G.M. and Everett K.R. 1989. The effect of nutrient and water additions on elemental mobility through small tundra watersheds. Holarctic Ecol. 12: 317–323.

Marion G.M. and Oechel W.C. 1993. Mid- to late-Holocene carbon balance in arctic Alaska and its implications for future global warming. The Holocene 3: 193–200.

Matthes-Sears U., Matthes-Sears W.C., Hastings S.J. and Oechel W.C. 1988. Variation in nutrient status, biomass, vegetative characteristics, and gas exchange of two deciduous shrubs on an arctic tundra slope. Arctic Alpine Res. 20: 342–351.

McGuire A.D., Melillo J.M., Joyce L.A., Kicklighter D.W., Grace A.L., Moore B. III and Vorosmarty C.J. 1992. Interactions between carbon and nitrogen dynamics in estimating net primary productivity for potential vegetation in North America. Global Biogeochem. Cycles 6: 101–124.

McGuire A.D., Clein J.S., Melillo J.M., Kicklighter D.W., Meier R.A., Vorosmarty C.J. and Serreze M.C. 2000. Modelling carbon responses of tundra ecosystems to historical and projected climate: sensitivity of Pan-Arctic carbon storage to temporal and spatial variation in climate. Global Change Biol. 6: 141–159.

McKane R.B., Rastetter E.B., Melillo J.M., Shaver G.R., Hopkinson C.S., Fernandes D.N., Skole D.L. and Chomentowski W.H. 1995. Effects of global change on carbon storage in tropical forests of South America. Global Biogeochem. Cycles 9 (3): 329–350.

McKane R.B., Rastetter E.B., Shaver G.R., Nadelhoffer K.J., Giblin A.E., Laundre J.A. and Chapin F.S. III. 1997a. Climatic effects on tundra carbon storage inferred from experimental data and a model. Ecology. 78: 1170–1187.

McKane R.B., Rastetter E.B., Shaver G.R., Nadelhoffer K.J., Giblin A.E., Laundre J.A. and Chapin F.S. III. 1997b. Reconstruction and analysis of historical changes in carbon storage in arctic tundra. Ecology 78: 1188–1198.

Mitchell J.F.B., Johns T.C., Gregory J.M. and Tett S.F.B. 1995. Climate response to increasing levels of greenhouse gases and sulphate aerosols. Nature 376: 501–504.

Moorhead D.L. and Reynolds J.F. 1993. Effects of climate change on decomposition in arctic tussock tundra: a modeling synthesis. Arct. Alp. Res. 25: 403–412.

Nadelhoffer K.J., Giblin A.E., Shaver G.R. and Linkins A.E. 1992. Microbial processes and plant nutrient availability in arctic soils. In: Chapin F.S. III, Jefferies R.L., Reynolds J.F., Shaver G.R., Svoboda J. (eds) Arctic Ecosystems in a Changing Climate: An Ecophysiological Perspective. Academic Press, San Diego, pp. 281–300

Nadelhoffer K.J., Shaver G.R., Giblin A.E. and Rastetter E.B. 1997. Potential impacts of climate change on nutrient cycling, decomposition, and productivity in Arctic ecosystems. In: Oechel W.C., Callaghan T., Gilmanov T., Holten J.I., Maxwell B., Molau O. and Sveinbjörnsson B. (eds) Global Change and Arctic Terrestrial Ecosystems. Springer, New York, pp. 349–364.

Newbold J.D., Elwood J.W., O'Neill R.V. and Van Winkle W. 1981. Measuring nutrient spiraling in streams. Can. J. Fish. Aquat. Sci., 38: 860–863.

Newbold J.D., O'Neill R.V., Elwood J.W. and Van Winkle W. 1982. Nutrient spiraling in streams: implications for nutrient limitation and invertebrate activity. Am. Nat. 120: 628–652.

Oberbauer S.F., Hastings S.J., Beyers J.L. and Oechel W.C. 1989. Comparative effects of downslope water and nutrient movement on plant nutrition, photosynthesis, and growth in Alaskan tundra. Holarctic Ecol. 12: 324–334.

Oechel W.C., Riechers G.H., Lawrence W.T., Prudhomme T.I., Vourtilis G.L., Grulke N. and Hasting S.J. 1992. 'CO2LT' an automated, null-balance system for studying the effects of elevated CO_2 and global change on unmanaged ecosystems. Funct. Ecol. 6: 86–100.

Ostendorf B. and Reynolds J.F. 1993. Relationships between a terrain-based hydrologic model and patch-scale vegetation patterns in an arctic tundra landscape. Landscape Ecol. 8: 229–237.

Ostendorf B., Quinn P., Beven K. and Tenhunen J.D. 1996. Hydrological controls on ecosystem gas exchange in an arctic landscape. In: Reynolds J.F. and Tenhunen J.D. (eds) Landscape Function and Disturbance in Arctic Tundra. Ecological Studies, Vol. 120. Springer-Verlag, Berlin, Heidelberg, pp. 369–386

Preedy N., McTiernan K., Matthews R., Heathwaite L. and Haygarth P. 2001. Rapid incidental phosphorus transfers from grassland. J. Environ. Qual. 30: 2105–2112.

Priestley C.H.B. and Taylor R.J. 1972. On the assessment of surface heat flux and evaporation using large-scale parameters. Monthly Weather Rev. 100: 81–92.

Rastetter E.B. 1996. Validating models of ecosystem response to global change. BioScience 46 (3): 190–198.

Rastetter E.B., Ryan M.G., Shaver G.R., Melillo J.M., Nadelhoffer K.J., Hobbie J.E. and Aber J.D. 1991. A general biogeochemical model describing the responses of the C and N cycles in terrestrial ecosystems to changes in CO2, climate and N deposition. Tree Physiol. 9: 101–126.

Rastetter E.B., McKane R.B., Shaver G.R. and Melillo J.M. 1992. Changes in C storage by terrestrial ecosystems: how C–N interactions restrict responses to CO2 and temperature. Water Air Soil Pollut. 64: 327–344.

Rastetter E.B., McKane R.B., Shaver G.R., Nadelhoffer K.J. and Giblin A.E. 1997. Analysis of CO_2, temperature, and moisture effects on carbon storage in Alaskan arctic tundra using a general ecosystem model. In: Oechel W.C., Callaghan T., Gilmanov T., Holten J.I., Maxwell B., Molau U. and Sveinbjörnsson B. (eds) Global Change and Arctic Terrestrial Ecosystems Springer-Verlag, New York, pp. 437–451.

Reiners W.A. and Driese K.L. 2001. The propagation of ecological influences through heterogeneous environmental space. BioScience 51: 939–950.

Reiners W.A., Keller M. and Gerow K.G. 1998. Nitrous oxide and methane fluxes across forest and pasture landscapes in Costa Rica. Water Air Soil Pollut. 105: 117–130.

Schimel D.S. 1990. Biogeochemical feedbacks in the earth system. In: Leggett J. (ed) Global Warming: The Greenhouse Report. Oxford University Press, Oxford, pp. 68–82.

Schimel J.P., Kielland K. and Chapin F.S. III 1996. Nutrient availability and uptake by tundra plants.In: Reynolds J.F. and Tenhunen J.D. (eds) Landscape Function and Disturbance in arctic Tundra. Ecological studies, Vol. 120, Springer-Verlag Berlin Heidelberg, pp. 203–221

Schloss A.L., Kicklighter D.W., Kaduk J., Wittenberg U. andthe participants of the Potsdam NPP model intercomparison. 1999. Comparing global models of terrestrial net primary productivity (NPP): comparison of NPP to climate and the Normalized Difference Vegetation Index (NDVI). Global Change Biol. 5 (Suppl. 1): 25–34.

Shaver G.R. and Chapin F.S. III 1986. Effect of fertilizer on production and biomass of tussock tundra, Alaska, USA. Arctic Alpine Res. 18: 261–268.

Shaver G.R. and Chapin F.S. III 1991. Production: biomass relationships and element cycling in contrasting arctic vegetation types, Ecol. Monogr. 61: 1–31.

Shaver G.R., Nadelhoffer K.J. and Giblin A.E. 1991. Biogeochemical diversity and element transport in a heterogeneous landscape, the North Slope of Alaska. In: Turner M.G. and Gardner R.H. (eds) Quantitative Methods in Landscape Ecology. Springer-Verlag, New York, pp. 105–126.

Shaver G.R., Billings W.D., Chapin F.S., Giblin A.E., Nadelhoffer K.J., Oechel W.C. and Rastetter E.B. 1992. Global change and the carbon balance of arctic ecosystems. Bioscience 42: 433–441.

Stieglitz M.Hobbie J.E., Giblin A.E. and Kling G. 1999. Hydrologic modeling of an Arctic Watershed: towards Pan-Arctic predictions. JGR Atmos 104 (D22): 27507–27518.

Sturm M., Racine C. and Tape K. 2001. Increasing shrub abundance in the Arctic. Nature 411: 546–547.

White J.D., Running S.W., Thornton P.E., Keane R.E., Ryan K.C., Fagre D.B. and Key C.H. 1998. Assessing simulated ecosystem processes for climate variability research at Glacier National Park, USA. Ecol. Appl. 8 (3): 805–823.

Williams M., Rastetter E.B., Shaver G.R., Hobbie J.E., Carpino E. and Kwiatkowski B.L. 2001. Primary production in an arctic watershed; an uncertainty analysis. Ecol. Appl. 11: 1800–1816.

Wilson K.B., Baldocchi D.D., Aubinet M., Berbigier P., Bernhofer C., Dolman H., Falge E., Field C., Goldstein A., Granier A., Grelle A., Halldor T., Hollinger D., Katul G., Law B.E., Lindroth A., Meyers T., Moncrieff J., Monson R., Oechel W., Tenhunen J., Valentini R., Verma S., Vesala T. and Wofsy S. 2002. Energy partitioning between latent and sensible heat flux during the warm season at FLUXNET sites. Water Resour. Res. 38 (12): 1294, doi 10.1029/2001WR000989.

Young P. 1984. Recursive Estimation and Time-Series Analysis. Springer-Verlag, Berlin 299 pp.